ACS Biomaterials SCIENCE & ENGINEERING

pubs.acs.org/journal/abseba

Article

Engineering Aligned Skeletal Muscle Tissue Using Decellularized Plant-Derived Scaffolds

Ya-Wen Cheng, Daniel J. Shiwarski, Rebecca L. Ball, Kathryn A. Whitehead, and Adam W. Feinberg*

Cite This: *ACS Biomater. Sci. Eng.* 2020, 6, 3046−3054

Read Online

ACCESS | Metrics & More | Article Recommendations

ABSTRACT: To achieve organization and function, engineered tissues require a scaffold that supports cell adhesion, alignment, growth, and differentiation. For skeletal muscle tissue engineering, decellularization has been an approach for fabricating 3D scaffolds that retain biological architecture. While many decellularization approaches are focused on utilizing animal muscle as the starting material, decellularized plants are a potential source of highly structured cellulose-rich scaffolds. Here, we assessed the potential for a variety of decellularized plant scaffolds to promote mouse and human muscle cell alignment and differentiation. After decellularizing a range of fruits and vegetables, we identified the green-onion scaffold to have appropriate surface topography for generating highly confluent and aligned C2C12 and human skeletal muscle cells (HSMCs). The topography of the green-onion cellulose scaffold contained a repeating pattern of grooves that are approximately 20 μm wide by 10 μm deep. The outer white section of the green onion had a microstructure that guided C2C12 cell differentiation into aligned myotubes. Quantitative analysis of C2C12 and HSMC alignment revealed an almost complete anisotropic organization compared to 2D isotropic controls. Our results demonstrate that the decellularized green onion cellulose scaffolds, particularly from the outer white bulb segment, provide a simple and low-cost substrate to engineer aligned human skeletal muscle.

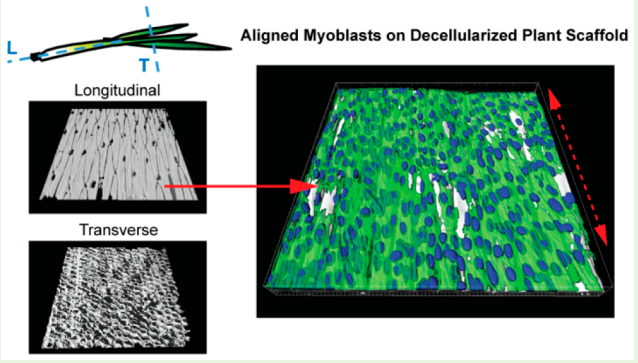

KEYWORDS: *engineered tissues, human skeletal muscle, decellularization, plant scaffolds*

INTRODUCTION

Damage to skeletal muscle and subsequent loss of function due to aging, trauma, and disease has spurred the development of new tissue engineering and regenerative medicine approaches.[1−3] Significant focus has been directed toward engineering the extracellular matrix (ECM), which plays a crucial role not only in the maintenance of muscle structure in vivo but also in the regenerative process by guiding cell migration, differentiation, and growth factor signaling.[4,5] However, identifying the critical factors that control these processes has been difficult because skeletal muscle tissue is highly complex, consisting of a collagen-rich ECM together with contractile myotubes, nerve fibers, and blood vessels.[4,6] What is known is that uniaxial alignment of myoblasts and fusion into multinucleated myotubes is critical to promote contractile function.[7,8] When cultured on a 2D surface or in a 3D hydrogel myoblasts can still fuse, however, without additional signals or information within the microenvironment the myotubes are unable to align with each other and thus form an isotropic network of poorly organized muscle.[9−12]

A number of approaches have been developed to engineer biomaterial scaffolds to guide muscle formation by integrating structural, mechanical, and chemical cues. In vitro studies using microengineered substrates have shown that unidirectional alignment of myotubes is required for the maximal generation of contractile force.[13,14] Specifically, substrate stiffness, ECM protein micropatterning, and surface microtopography all affect myoblast alignment and fusion into myotubes.[13,15,16] Similar results have been observed using decellularized tissue scaffolds, where detergents are used to remove the cells but preserve the structural, biochemical, and biomechanical properties of the native ECM.[2] Decellularized tissue scaffolds have proved to be an effective strategy for engineering both cardiac[17−19] and skeletal muscle[20−23] to create aligned tissues. While these approaches can be used to engineer muscle, they rely on either specialized and costly microfabrication processes or perfusion decellularization of volumetric muscle tissue. Recently, plants

Received: January 12, 2020
Accepted: March 10, 2020
Published: March 10, 2020

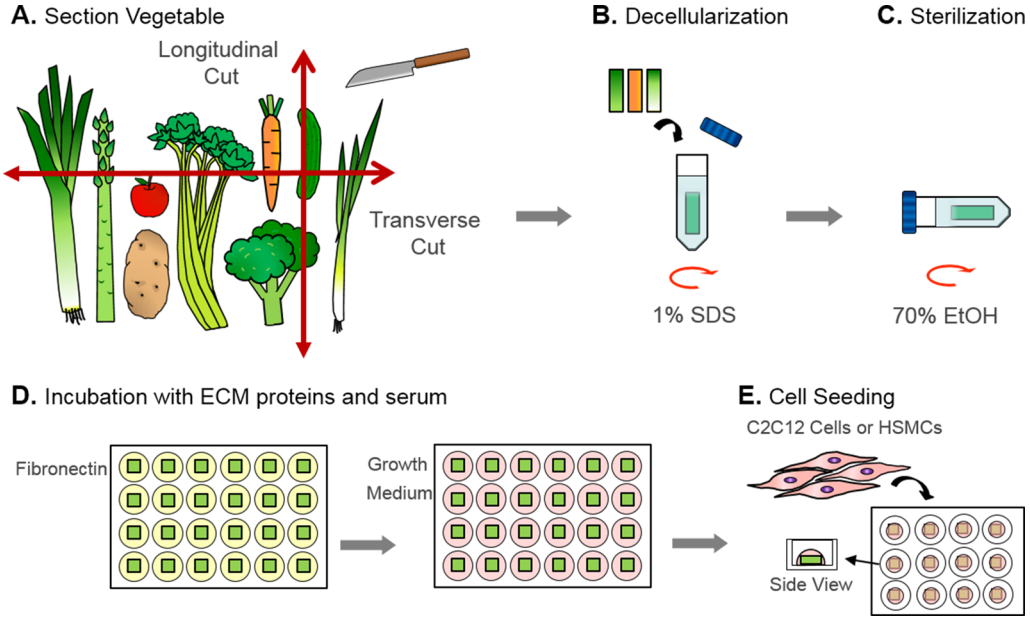

Figure 1. Preparation, decellularization, and seeding of plant-derived cellulose scaffolds. (A) A selection of fruits and vegetables was chosen to serve as cellulose scaffold substrates to enhance the growth and alignment of human muscle cells. Each sample was cut longitudinally and transversely into 1−2 mm slices. (B) For decellularization, the sectioned samples were placed in 1% (w/v) at 25 °C for 3 weeks. (C) After decellularization, plant tissues were sterilized with 70% EtOH for 1 h and stored at 4 °C. (D) Sterile scaffolds were incubated with fibronectin (50 μg/mL) solution in a 24-well plate at 37 °C overnight. Following fibronectin coating, serum containing growth medium was used to condition the scaffolds at 37 °C overnight before plating of cells. (E) C2C12 or HSMCs cells were seeded on top of the protein absorbed scaffolds in a 12-well plate. Following cell attachment, more culture medium was added and cells were cultured for 5−7 days.

have been identified as an alternative source for decellularized scaffolds that are inexpensive, abundantly available, and yield 3D cellulose structures that can support mammalian cell growth. For example, apple and parsley stems retain their complex structure, and the vascular-like network in vanilla and spinach leaves can be used to template a vascular network, with potential application in perfusing larger engineered tissues.[24−26] The use of scaffolds derived from common fruits or vegetables with architectures uniquely suited for muscle alignment could offer a more broadly accessible and inexpensive alternative to other approaches.

The goal of this study was to leverage the unique cellulose structures and topographies of common fruits and vegetables to create a low-cost scaffold that guides myoblast alignment and enables the engineering of organized muscle tissue. Plants, including fruits and vegetables, offer a broad range of potential cellulose architectures and surface topographies for this purpose. Specifically, we sought to identify a simple and low-cost, plant-derived scaffold that enables the alignment of human myoblasts into highly aligned myotubes in 2D. To do this, we examined nine sources of plant scaffolds, including carrot, broccoli, cucumber, potato, apple, asparagus, green onion, leek, and celery. Upon decellularization with a sodium dodecyl sulfate (SDS) solution, we obtained cellulose scaffolds with varied pore diameters, aspect ratios, and degrees of anisotropy. We determined that coating the scaffolds with fibronectin improved adhesion and analyzed the alignment of C2C12 myoblasts and human skeletal myoblasts (HSMCs) seeded on top of the scaffolds. The green onion-derived cellulose scaffold was the best topography for C2C12 attachment and differentiation into aligned myotubes and the outside of the white bulb of the green onion enabled HSMCs to form an aligned monolayer of differentiated myotubes. These results show that the decellularized green onion cellulose scaffolds can act as a low-cost biocompatible biomaterial for muscle tissue engineering because of their anisotropic micropattern topography to drive muscle cell alignment and formation.

MATERIALS AND METHODS

Materials. C2C12 cells were obtained from ATCC (catalog no. CRL-1772). Fibronectin was bought from Corning (catalog no. 354008). Paraformaldehyde aqueous solution was purchased from Electron Microscopy Sciences, Inc. (catalog no. 15710). TrypLE Express (catalog no. 12604013), NucGreen Dead 488 (catalog no. R37109), myosin heavy chain antibody (catalog no. MS-1177-RQ), Triton X-100 (catalog no. 28313), Alexa Fluor 555 conjugated phalloidin (catalog no. A34055), Alexa Fluor 633 goat antimouse secondary antibody (catalog no. A-21052), and Pro-Long Gold Antifade reagent (catalog no. P36934) were bought from Thermo Fisher Scientific. Calcofluor White M2R (catalog no. 18909) and SDS (catalog no. L3771) were purchased from Sigma-Aldrich.

Fruit and Vegetable Decellularization. Fruits and vegetables including carrot, broccoli, cucumber, potato, apple, asparagus, green onion, leek, and celery were purchased from local supermarkets (Pittsburgh, PA) and stored at 4 °C. To assess the microscale cellulose architecture, the fruits and vegetables were cut longitudinally or transversely into 1−2 mm thick slices (Figure 1A), submerged in 1% (w/v) SDS and shaken at 70 rpm at 25 °C for 3 weeks, with the 1% (w/v) SDS solution refreshed weekly (Figure 1B). Decellularized slices were then fixed and stained for cellulose (Calcofluor White M2R, Sigma-Aldrich), and nuclei (NucGreen Dead 488, Thermo Fisher). The decellularization process was considered complete when no nuclei were observed following confocal microscopy. After decellularization, the samples were washed twice with phosphate buffered saline (PBS) at 60 rpm and then incubated with 1% streptomycin/penicillin in PBS at 60 rpm overnight. All samples were stored at 4 °C for no more than one month before use.

Preparation of Sterile, Functionalized Scaffolds. Decellularized plant tissues were cut into 0.5 × 0.5 cm size scaffolds with a scalpel. For sterilization, the decellularized scaffolds were incubated

https://dx.doi.org/10.1021/acsbiomaterials.0c00058
ACS Biomater. Sci. Eng. 2020, 6, 3046−3054

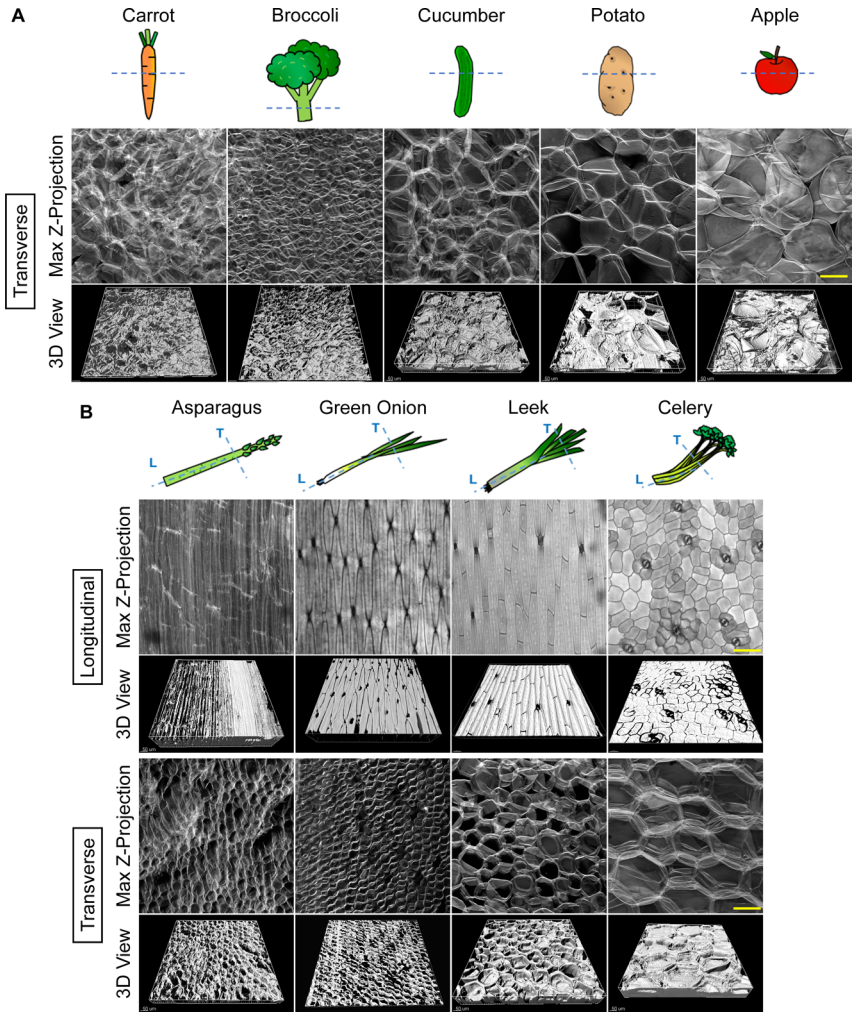

Figure 2. Decellularized cellulose scaffolds of vegetables and fruits reveal distinct isotropic and anisotropic architecture. (A) Vegetable and fruit sections were acquired in the orientation depicted by the dotted line, decellularized, stained for cellulose using Calcofluor White, and imaged via confocal fluorescence microscopy. The scaffolds derived from carrot, broccoli, cucumber, potato, and apple exhibited isotropic cellulose structures when cutting in both longitudinal (L) and transverse (T) direction (scale bar = 100 μm). (B) For both transverse, and longitudinal preparations, anisotropic cellulose structures were identified in asparagus, green onion, leek, and celery (scale bar = 100 μm). The three-dimensional reconstruction of the cellulose scaffolds is shown below each fluorescence image (scale bar = 50 μm).

with 70% EtOH on a shaker at 70 rpm for 1 h in a 50 mL conical tube (Figure 1C). Scaffolds were then rinsed with sterile PBS ten times and gently shaken for 30 s each rinse. Sterile cellulose scaffolds were incubated with human fibronectin (Corning) at 50 μg/mL in a 24-well plate at 37 °C overnight (Figure 1D). The fibronectin solution was removed, and the samples were incubated with standard C2C12 growth medium consisting of high glucose DMEM (Corning) supplemented with 10% fetal bovine serum, 1% penicillin-streptomycin, and 1% L-glutamine (200 mM) overnight at 37 °C in a humidified cell culture incubator.

C2C12 Cell Culture and Differentiation. C2C12 mouse myoblasts were cultured at 37 °C and 10% CO_2 and passaged at 80% confluence. Cells were seeded on to protein-incubated scaffolds by pipetting 40 μL of 20 000 cells/scaffold in a nontreated cell culture 12-well plate (Figure 1E) and incubated for 6 h. Following cell attachment, 3 mL of culture medium was added to the samples and medium was changed every other day. For control samples, glass coverslips were UV-ozone treated for 15 min, incubated with fibronectin (50 μg/mL) for 30 min, washed with PBS and then seeded with 20 000 cells/coverslip. For differentiation of the C2C12 cells, the culture medium was exchanged with differentiation medium consisting of high glucose DMEM supplemented with 2% horse serum, 1% penicillin-streptomycin, and 1% L-glutamine (200 mM) after 3 days. Subsequent media exchanges occurred every other day for 6 days. After differentiation, scaffolds were fixed and prepared for immunofluorescence.

Human Skeletal Muscle Cell (HSMC) Culture. Human skeletal myoblasts (HSMCs) were obtained from Cook Myosite (catalog no. SK-1111). Growth and differentiation were performed according to the manufacturer's published guidelines at 37 °C and 5% CO_2. Briefly, HSMCs were grown in myotonic growth media (Cook Myosite; catalog no. MK-4444), subcultured at 60% confluence, passed at a ratio of 1:3, and used at passage numbers less than 10. The HSMCs were seeded on top of protein-incubated scaffolds at 20 000 cells/scaffold in a nontreated cell culture 12-well plate. The plate was placed in an incubator for 6 h. Following cell attachment, 3 mL of growth medium + 1% penicillin−streptomycin was added to the samples and media was refreshed every other day. For control samples, glass coverslips were UV−ozone-treated for 15 min, incubated with fibronectin (50 μg/mL) for 30 min, washed with PBS, and then, seeded with 20 000 cells/coverslip. For differentiation of the HSMCs, the growth medium was replaced by myotonic differentiation media (Cook Myosite; catalog no. MD-5555) + 1% penicillin−streptomycin after 3 days. Subsequent media exchanges occurred every other day for 6 days. After differentiation, scaffolds were fixed and prepared for immunofluorescence analysis.

Immunofluorescent Staining and Image Analysis. For immunofluorescent staining, the scaffolds were rinsed with PBS and

https://dx.doi.org/10.1021/acsbiomaterials.0c00058
ACS Biomater. Sci. Eng. 2020, 6, 3046−3054

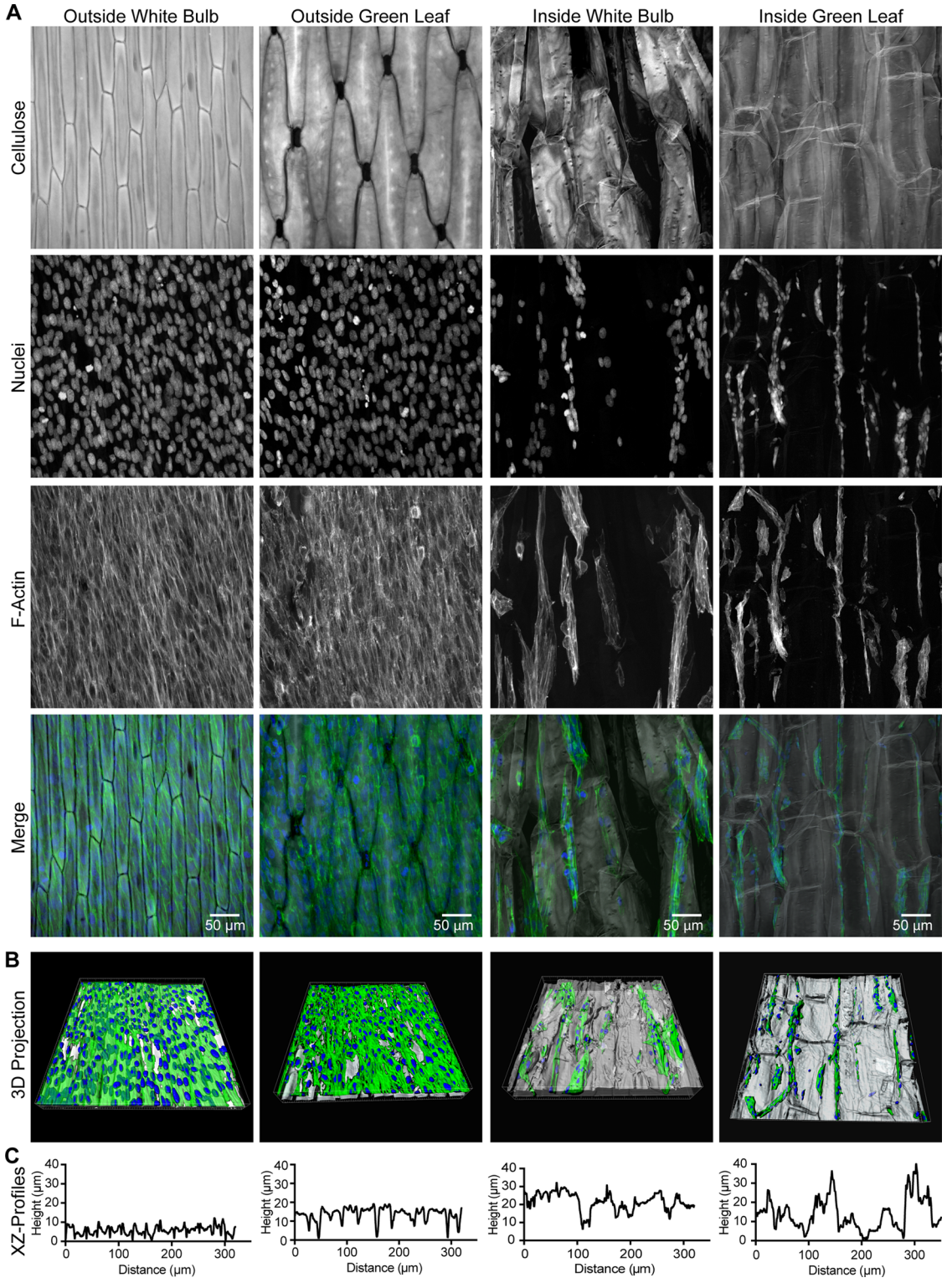

Figure 3. C2C12 cells adhere and proliferate on the outer cellulose scaffolds of the green onion bulb and leaf. The anisotropy of the green onion leads to its use for cellularization studies. Different surface microstructures and topology from separate parts of the green onion were incubated with fibronectin and seeded with C2C12 cells. (A) Cellulose scaffolds from the interior and exterior green onion white bulb and green leaf were preincubated with fibronectin (50 μg/mL) and fetal bovine serum for 24 h before cell seeding. C2C12 cells were seeded to either the inner or outer white bulb and green leaf surfaces. The samples were then fixed and stained for confocal immunofluorescence analysis of the cellulose scaffold (Calcofluor White, gray), nuclei (NucGreen 488, blue), F-Actin (Phalloidin, green) to view cell growth and attachment. (B) Three-dimensional reconstructions of the respective green onion scaffolds show a cell preference for the anisotropic and shallow topology of the outside of the white bulb and green leaf (cellulose scaffold, Calcofluor White, gray; nuclei, NucGreen 488, blue; F-actin, phalloidin, green). (C) Cross-section *XZ* profiles of the surface topography of the scaffolds orthogonal to the direction of alignment, generated from the 3D confocal *z*-stacks of the Calcofluor White stained cellulose.

https://dx.doi.org/10.1021/acsbiomaterials.0c00058
ACS Biomater. Sci. Eng. 2020, 6, 3046−3054

fixed with 4% paraformaldehyde with 0.05% of Triton X-100 for 15 min. Samples were then rinsed three times with PBS on a shaker for 5 min each. Afterward, samples were incubated with 1:100 dilution of mouse monoclonal alpha myosin heavy chain (αMHC) antibody overnight at room temperature to visualize myotube formation. Samples were rinsed three times with PBS and incubated overnight with NucGreen 488 for nucleus staining, 1:10 000 Calcofluor White M2R to stain the cellulose, 1:100 dilution of Alexa Fluor 555 conjugated phalloidin for actin staining, and 1:1000 dilution of Alexa Fluor 633 goat antimouse secondary antibody. Samples were rinsed three times in PBS, mounted using Pro-Long Gold Antifade reagent, and imaged at 20× magnification on a Zeiss LSM 700 laser scanning confocal microscope to obtain 3D reconstructions of the cell-laden scaffolds.

To quantify the actin alignment of cells on cellulose scaffolds, a 2D orientation order parameter (OOP) was calculated from maximum intensity *z*-projections of confocal image stacks, based on established methods.[27,28] Briefly, maximum intensity *z*-projections were imported into MATLAB and the direction of actin filaments was identified and an orientation angle assigned for each pixel in the images. These orientation angles were then used to calculate the orientation order parameter for each sample. The OOP ranges from 0 to 1, where 1 corresponds to perfect anisotropic orientation (e.g., complete uniaxial alignment), while 0 indicates fully isotropic orientation. For each experimental condition, the OOP values for individual scaffolds indicate the ability of the cellulose scaffold to induce cellular alignment compared to cells grown on a uniform coated coverglass control.

Statistics and Data Analysis. Image analysis and figure preparation were performed using ImageJ and Adobe Photoshop CS6. Graphing and statistical analyses were performed using Graphpad Prism 6. A minimum of three independent experiments were performed for each set of data. For statistical analysis of the OOP, a one-way ANOVA was performed followed by Dunn's Multiple Comparison Test. A p-value of <0.05 was considered statistically significant.

RESULTS

Evaluation of Fruit and Vegetable Cellulose Structures. We began by screening a selection of nine fruits and vegetables for the ability of their intrinsic cellulose structure to induce muscle cell alignment. We evaluated carrots, broccoli, cucumber, potato, apple, asparagus, green onion, leek, and celery (Figure 1). Two types of slices were evaluated from each fruit or vegetable following either a longitudinal or a transverse cut (Figure 1A). The slices, which were 1−2 mm thick, were placed into 1% (w/v) SDS on an orbital shaker for 3 weeks to remove the plant cellular content (Figure 1B). After decellularization, the samples were stained with Calcofluor White and imaged via fluorescence confocal microscopy to examine the cellulose structures in the longitudinal and transversal directions. For cell growth studies, scaffolds were sterilized (Figure 1C) before being coated with fibronectin and incubated in growth medium (Figure 1D). Finally, cells were seeded on scaffolds for growth and alignment assessment (Figure 1E).

Decellularized cellulose scaffolds of vegetables and fruits exhibited distinct architectures ranging from isotropic to anisotropic. The cellulose scaffolds derived from carrot, broccoli stalk, cucumber, potato, and apple presented interwoven circular structures of varying sizes (Figure 2A). The circular structures in carrot and broccoli stalks were 30−40 μm in diameter, while in cucumber, it was approximately 100 μm in diameter, and in potato and apple, they were 200−300 μm. These five samples displayed isotropic cellulose structures, meaning the architecture was similar in transverse and longitudinal directions. By contrast, cellulose scaffolds derived from asparagus, green onion, leek, and celery exhibited anisotropic structures with dissimilar structures when cut longitudinally versus transverse (Figure 2B). Specifically, the longitudinal cuts for asparagus, green onion, and leek showed highly aligned architectures reminiscent of microengineered surfaced shown to facilitate myoblast differentiation and myotube alignment.[13,14] Based on this, we hypothesized that the anisotropic structures found in the longitudinal direction of the asparagus, green onion, and leek could direct growth and alignment of skeletal muscle. Specifically, we chose to move forward with green onion because its scaffold dimensions offered the flattest surface for cell culture and attachment, together with a high aspect ratio of the surface structures for guiding cell alignment.

Myoblast Cells Proliferated on Green Onion Scaffolds. There are two main sections of the green onion plant: the white bulb and the green leaf, which are easily distinguished based on their color, texture, and locations on opposite ends of the plant. We hypothesized that the white bulb and green leaf segments would yield different cellulose scaffold surfaces that would influence cell attachment and alignment. As such, we examined the cellulose structure of the four distinct surfaces of the entire green onion plant in more detail.

Because onions have a layered structure, each section of the plant leaf possesses inward-facing (inner) and outward-facing (outer) surfaces. These four surfaces of the green onion plant—outer white bulb, outer green leaf, inner white bulb, and inner green leaf—were isolated by cutting small sheets of vegetable from the appropriate location. To examine the cellulose scaffold architecture, these sheets were then decellularized, stained with Calcofluor White, and imaged via fluorescence confocal microscopy. Clear differences in cellulose structure were observed for the four green onion surfaces (Figure 3A, top row), with the outer white bulb featuring the smallest dimensions, and the inner surfaces being the most disordered.

To determine whether green onion cellulose scaffolds could promote muscle tissue formation, we seeded and cultured C2C12 cells onto four green onion-derived cellulose scaffolds (Figure 3A). After 3 days, the outer surfaces supported the growth of a C2C12 cell monolayer with 80−90% confluence, whereas the inner surfaces resulted in low cell adhesion with minimal proliferation. Three-dimensional reconstruction of the confocal images enabled the calculation of the height of the scaffold pores as a function of location in the *XY* plane (Figure 3B). Confocal *XZ* image projections were then used to create a *Z*-axis profile plot to demonstrate the variations in scaffold surface topology for each sample. (Figure 3C). The topography of the outer white bulb-derived scaffold was highly uniform with a unit cell structure defined by an edge height of approximately 12 μm with an inner groove of 20−30 μm in width and less than 10 μm in depth. The topography of the outer green leaf-derived scaffold was also highly uniform, with a repeating unit structure defined by shallow edge grooves that were approximately 9 μm wide and 10−15 μm deep, followed by a 20 μm tall plateau with a width of 50 μm. By comparison, the inner surfaces were rougher and less defined. The peak height for the inner white bulb topography was 26 μm and the inner green leaf structure was 40 μm. The edge grooves of the inner white bulb surface were 25−60 μm in width and 15−25 μm in depth, while the grooves of the inner green leaf surface

https://dx.doi.org/10.1021/acsbiomaterials.0c00058
ACS Biomater. Sci. Eng. 2020, 6, 3046−3054

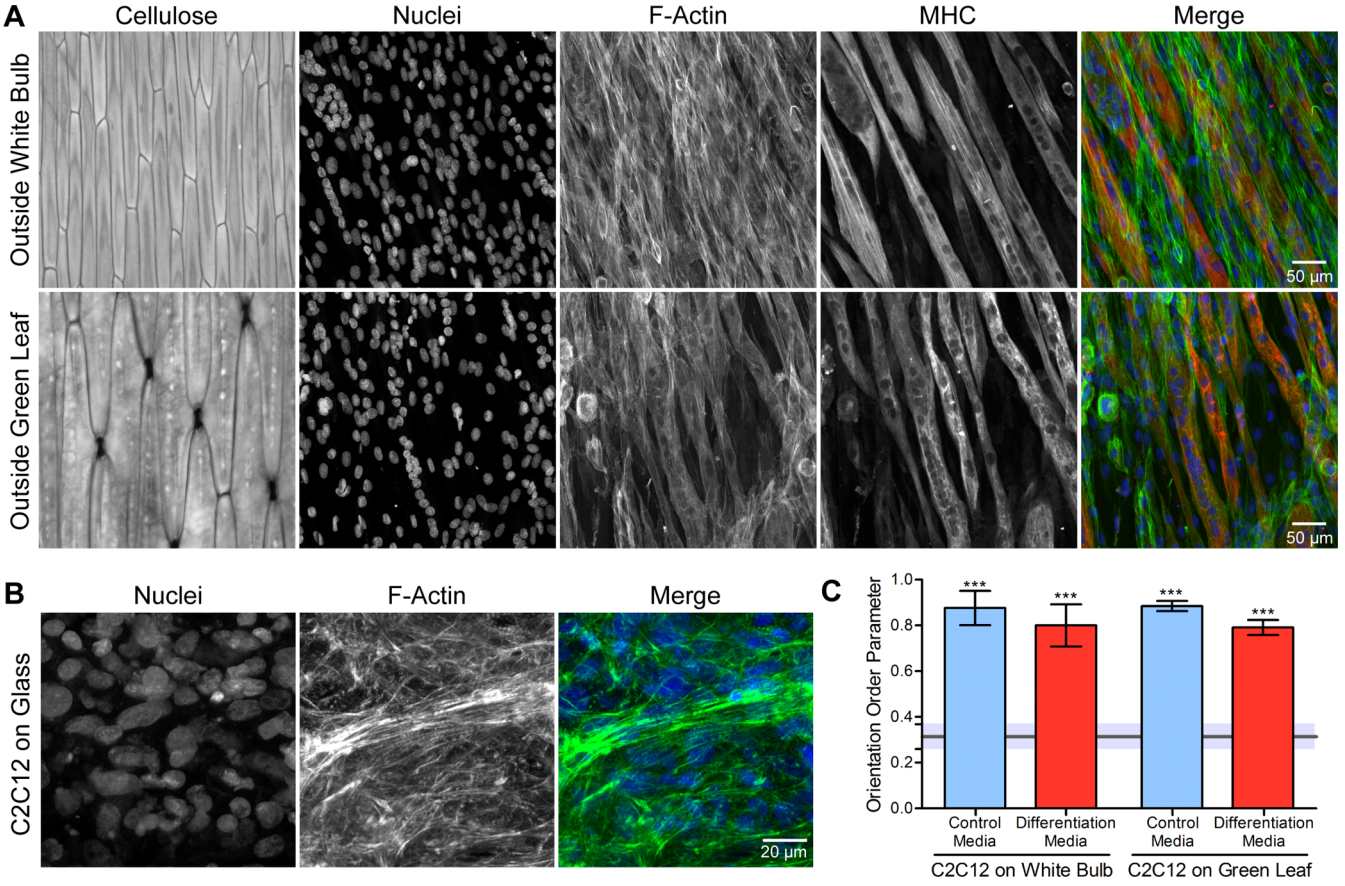

Figure 4. C2C12 cells differentiate into aligned myotubes when cultured on the outer surface of the green onion derived cellulose scaffolds. (A) When cultured on the outer green onion white bulb or green leaf cellulose scaffolds, C2C12 cells preferentially align uniaxially and move in the direction of the cellulose scaffold topology as measured by myotube expression (nuclei, NucGreen 488, blue; F-actin, phalloidin, green; myotubes, αMHC, red; scale bar = 50 μm). (B) Example confocal fluorescence image showing C2C12 cells align randomly when cultured on a fibronectin-coated (50 μg/mL) glass coverslip (nuclei, NucGreen 488, blue; F-actin, phalloidin, green; scale bar = 20 μm). (C) Quantitative analysis of the fluorescence images obtained for actin alignment is performed via a 2D orientation order parameter (OOP) of C2C12 cells seeded on various substrates. In control conditions, when C2C12 cells are plated onto glass coverslips, a low OOP is observed due to a lack of cellular alignment (OOP = 0.31). In both the control medium condition and differentiated conditions, C2C12 cells seeded onto the cellulose scaffolds of the outer green onion white bulb and green leaf surfaces displayed a highly aligned OOP. For each condition, either before or after differentiation, the C2C12 cells on the green onion scaffolds showed a significant increase in OOP compared to the control cells seeded on glass coverslips (n = 6–10; *** = P < 0.001 compared to C2C12 on glass control).

were 50–150 μm wide and about 20–30 μm deep. On the basis of these data, we chose to move forward with the outer white bulb- and green leaf-derived scaffolds because of their uniform structure and ability to support cell attachment and growth.

Myoblast Cells Align on Green Onion-Derived Cellulose Scaffolds. For skeletal muscle to achieve adequate force generation and coordinated muscular contraction, myoblasts must align uniaxially.[13,14] Therefore, we next assessed the ability of the green onion cellulose scaffolds to enhance C2C12 myoblast cell alignment and promote the formation of contractile myotubes. After culturing C2C12 cells in growth medium on the outer green leaf and white bulb scaffolds for 3 days, the culture medium was exchanged for myoblast differentiation medium to stimulate cell differentiation and alignment. Following 6 days of differentiation, the scaffolds were fixed and cellular alignment and myotube formation were determined via fluorescence confocal microscopy. As a 2D isotropic control, C2C12 cells were grown on glass coverslips to determine their alignment. Cells grew and aligned on the outer white bulb- and green leaf-derived cellulose scaffolds (Figure 4A), whereas cells cultured on glass coverslips were randomly oriented (Figure 4B). The C2C12 cells were then differentiated into well-ordered myotubes, as indicated by the presence of αMHC.

Analysis of cell alignment showed that the OOP for C2C12 cells grown on glass coverslip controls was approximately 0.31 (n = 6), indicating poor alignment. The OOP of C2C12 cells grown on the outer surface of both bulb (n = 9) and leaf segments (n = 6) of the scaffolds before differentiation was approximately 0.9 (Figure 4C). The OOP of C2C12 cells grown on the outside surface of both bulb (n = 10) and leaf parts (n = 6) of the scaffolds after differentiation was approximately 0.8 (Figure 4C). Although the cell alignment dropped ~10% after differentiation, the data indicate that the C2C12 cells grew in a preferred orientation once they attached to the aligned surface of the cellulose scaffolds before differentiation. Taken together, these results confirm that decellularized green onion cellulose scaffolds can support C2C12 cell growth, attachment, and alignment of myotubes. The most well-aligned condition was achieved using the outer

https://dx.doi.org/10.1021/acsbiomaterials.0c00058
ACS Biomater. Sci. Eng. 2020, 6, 3046–3054

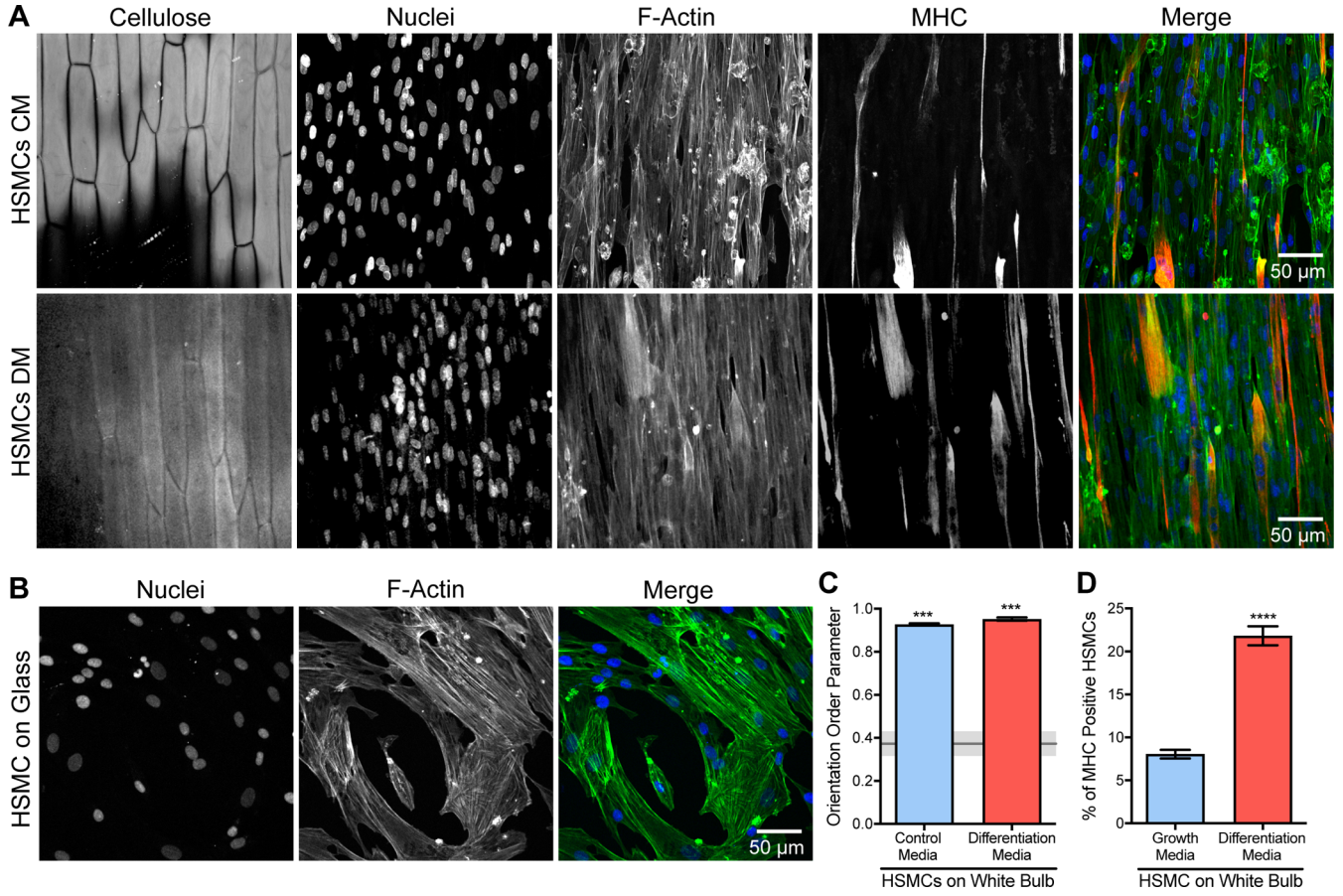

Figure 5. HSMCs differentiate into aligned myotubes when cultured on the outer surface of the green onion white bulb cellulose scaffolds. (A) When cultured on the outer green onion white bulb cellulose scaffolds, in either control medium (CM) or differentiation medium (DM), HSMCs highly align and differentiate in the direction of the cellulose scaffold topology (nuclei, NucGreen 488, blue; F-actin, phalloidin, green; myotubes, αMHC, red; scale bar = 50 μm). (B) Example confocal fluorescence image showing HSMCs align randomly when cultured on a fibronectin-coated (50 μg/mL) glass coverslip (nuclei, NucGreen 488, blue; F-actin, phalloidin, green; scale bar = 50 μm). (C) In control conditions, when HSMCs are plated onto glass coverslips, a low OOP is observed due to a lack of cellular alignment (OOP = 0.37). In both the control and differentiation medium conditions, HSMCs cells seeded onto the cellulose scaffolds of the outside green onion white bulb surfaces exhibited a highly aligned OOP approaching above 0.9. For each condition, either in control or differentiation medium, the HSMCs seeded on the green onion scaffolds showed a significant increase in OOP compared to the control cells seeded on glass coverslips (n = 6–10; *** = P < 0.001 compared to HSMCs on glass control). (D) The percentage of αMHC positive cells on white bulb scaffolds before and after switching from control to differentiation media were 8 ± 2% and 22 ± 5%, respectively (n = 20 fields for each, p < 0.0001).

white bulb cellulose scaffold. Therefore, this scaffold was chosen to engineer aligned human skeletal muscle tissue.

Human Skeletal Muscle Cells Align on Green Onion-Derived Cellulose Scaffolds. Finally, we sought to grow aligned and differentiated human skeletal muscle cells on the outer white bulb-derived green onion cellulose scaffolds. HSMCs were cultured and seeded following similar procedures to the C2C12 cells. HSMCs were seeded on glass coverslips (isotropic control) and on the outer green onion white bulb-derived scaffolds. Following 6 days of culture in myotonic growth media or myotonic differentiation media, the HSMC-seeded scaffolds were fixed. Scaffolds were then stained to examine cellular alignment and myotube formation (Figure 5A and 5B) and analyzed for OOP to quantify HSMC alignment (Figure 5C). HSMCs cultured on glass coverslips were observed to be randomly oriented (OOP = 0.37, n = 7), and HSMCs grown on the outer white bulb-derived cellulose scaffolds aligned almost perfectly (OOP = 0.95, n = 7). Furthermore, we observed HSMC myotube formation on the outer white bulb-derived cellulose scaffolds, as indicated by positive staining for αMHC following transition to differentiation media (Figure 5D).

DISCUSSION

On the basis of the 3D confocal imaging of various decellularized plant scaffolds, we identified the white bulb of the green onion as an architecture that can guide the alignment of mouse and human muscle cells. This is an important finding because it provides an accessible, low-cost approach for engineering aligned muscle fibers without requiring access to advanced microfabrication or whole organ decellularization technologies. The decellularized green-onion scaffolds contained aligned surface microstructures that directed C2C12 and HSMC cells to form a highly confluent monolayer on the scaffold. The unit cell microstructure of the white bulb of the green onion was composed of repeating grooves approxima 20 μm wide, 5 μm spaced, and 10 μm in depth. This structure provided a topographic pattern that was able to generate a uniform monolayer of aligned muscle cells. Since the diameter of the C2C12 cells are less than 10 μm and the HSMCs are

https://dx.doi.org/10.1021/acsbiomaterials.0c00058
ACS Biomater. Sci. Eng. 2020, 6, 3046–3054

approximately 10−25 μm,[29] the unit cell dimension of the green onion cellulose scaffold was well suited to induce uniaxial alignment. The C2C12 cell alignment was at a slight angle to the underlying topography of the outer white bulb scaffolds (Figure 4A). This is a unique response of C2C12s and this off-axis alignment has been previously reported for this cell type on different micropatterned substrates.[13,30−32]

Plant-derived decellularized cellulose scaffolds show promise as a biomaterial resource for tissue engineering applications. Our work to engineer aligned muscle cells provides an important contribution to the field. When decellularized apple hypanthium tissue was used to culture mammalian cell types, such as NIH 3T3, C2C12, and HeLa cells, the cells attached to the scaffolds but did not spread out well on the entire seeding surface.[24] Although it was confirmed that the cells could live on the scaffolds for 12 weeks, many cells aggregated in the hollow spaces of the cellulose structure. This suggested that the size and scale of the apple-derived cellulose scaffold microstructure was too large for mammalian cell growth and monolayer formation. Studies looking at the vasculature in spinach leaf-derived scaffolds showed the ability to support human pluripotent stem cell-derived cardiomyocytes (hPS-CMs) adhesion and survival. Specifically, it was shown that the hPS-CMs remained beating after 3 weeks; however, the cells appeared highly aggregated indicating that the cells were alive but not fully interacting with the scaffold surface adequately enough to spread and form a contractile monolayer.[25] In contrast, we demonstrate that the green onion derived cellulose scaffold has an anisotropic topography that can guide cell attachment, growth, differentiation, and myofibril alignment. Thus, we provide the first example of a plant-derived cellulose scaffold being sufficient to align muscle cells into a confluent monolayer. This suggests that repeating grooves with approxi 20 μm wide, 10 μm deep, and 5 μm spacing provide an appropriate topography to generate an aligned muscle cell monolayer. Typically the fabrication of 3D topographies at the micron scale requires advanced fabrication techniques, such as 3D printing, electrospinning, or microfabrication. The current resolution of 3D printing is around tens of microns, so the microstructures of the plant cellulose scaffolds would be challenging to replicate accurately via this method. Microfabrication should be able to manufacture the microgeometry, but it would require more expensive facilities and specialized processing equipment. Therefore, considering the fabrication time, cost, and resources required, decellularized plant scaffolds, such as our green onion-derived scaffold is a simple, low-cost, and abundant method to achieve the appropriate topography for uniformly aligned muscle cells.

When engineering a device or platform for translational applications, biocompatibility is usually the most critical barrier to overcome. For plant-derived cellulose scaffolds, although not extensively investigated, the biocompatibility appears promising. The apple-derived cellulose scaffold showed only a mild immune response when implanted subcutaneously.[33] Cellulose scaffolds built with isolated cellulose fibers also elicit a relatively moderate postimplantation immune response.[34] In addition to immune response, the degradation of the cellulose scaffold should also be considered. Since there are no cellulases in the human body, future investigations into the persistence of the plant-derived cellulose scaffolds and their impact on the regenerative capacity for tissue engineering applications will be needed. Some studies have confirmed that cellulase pretreatment of cellulose scaffolds, or tuning the composition of amorphous and crystalline cellulose could regulate the degradation period after implantation.[34−36] Another viable option is to treat the cellulose components in the scaffold in vitro with cellulase once the muscle cells grow and form a solid muscular tissue structure prior to implantation. This would allow the muscle cells to align and differentiate on the scaffold preimplantation, followed by removal of the cellulose structure before being implanted in the target tissue. While our data and others have demonstrated an important role for decellularized plant scaffolds in tissue engineering applications, more research is needed to translate this approach into a clinically relevant biomaterial with abundant and low-cost resources.

In conclusion, we show, that the decellularized green onion cellulose scaffolds, particularly from the outer white bulb segment, can both support and stimulate growth, proliferation, and differentiation of human skeletal muscle, while also providing the necessary alignment of myotubes required for enhanced functional contractility of muscle tissue. We conclude that a repeating groove with approxi 20 μm wide, 10 μm deep, and 5 μm spacing of plant-derived cellulose scaffold is an appropriate 3D microstructure for engineering human skeletal muscle tissue. This naturally derived structure agrees with our previously published work looking at muscle cell alignment following patterning fibronectin on topographic PDMS substrates.[13] By leveraging the readily available green onion cellulose scaffold, and SDS-based decellularization techniques, we have developed a low cost and effective platform for achieving high alignment of skeletal muscle for use in tissue engineering. For future applications in vivo, such as volumetric muscle loss, additional research will be required to maximize muscle differentiation on the scaffolds and to ensure complete decellularization in order to minimize the immune response that would occur due to xenogeneic plant-derived cellular debris.

AUTHOR INFORMATION

Corresponding Author

Adam W. Feinberg − *Department of Biomedical Engineering and Department of Materials Science & Engineering, Carnegie Mellon University, Pittsburgh, Pennsylvania 15213, United States*; orcid.org/0000-0003-3338-5456; Email: feinberg@andrew.cmu.edu

Authors

Ya-Wen Cheng − *Department of Biomedical Engineering and Department of Chemical Engineering, Carnegie Mellon University, Pittsburgh, Pennsylvania 15213, United States*

Daniel J. Shiwarski − *Department of Biomedical Engineering, Carnegie Mellon University, Pittsburgh, Pennsylvania 15213, United States*

Rebecca L. Ball − *Department of Chemical Engineering, Carnegie Mellon University, Pittsburgh, Pennsylvania 15213, United States*

Kathryn A. Whitehead − *Department of Biomedical Engineering and Department of Chemical Engineering, Carnegie Mellon University, Pittsburgh, Pennsylvania 15213, United States*; orcid.org/0000-0002-0100-7824

Complete contact information is available at: https://pubs.acs.org/10.1021/acsbiomaterials.0c00058

Notes

The authors declare no competing financial interest.

https://dx.doi.org/10.1021/acsbiomaterials.0c00058
ACS Biomater. Sci. Eng. 2020, 6, 3046−3054

■ ACKNOWLEDGMENTS

We thank Rachelle Palchesko and Ivan Batalov for assistance with experimental analysis and general guidance. Research reported in this publication was supported by the National Heart, Lung, and Blood Institute of the National Institutes of Health under Award Number F32HL142229 and DP2HL117750 and the Office of Naval Research under Award Number N00014-17-1-2566.

■ REFERENCES

(1) Tan, S. J.; Fang, J. Y.; Wu, Y.; Yang, Z.; Liang, G.; Han, B. Muscle tissue engineering and regeneration through epigenetic reprogramming and scaffold manipulation. *Sci. Rep.* **2015**, *5*, 16333.

(2) Gilpin, A.; Yang, Y. Decellularization Strategies for Regenerative Medicine: From Processing Techniques to Applications. *BioMed Res. Int.* **2017**, *2017*, 9831534.

(3) Duffy, R. M.; Feinberg, A. W. Engineered skeletal muscle tissue for soft robotics: fabrication strategies, current applications, and future challenges. *Wiley Interdisciplinary Reviews: Nanomedicine and Nanobiotechnology* **2014**, *6*, 178−195.

(4) Porzionato, A.; Sfriso, M. M.; Pontini, A.; Macchi, V.; Petrelli, L.; Pavan, P. G.; Natali, A. N.; Bassetto, F.; Vindigni, V.; De Caro, R. Decellularized Human Skeletal Muscle as Biologic Scaffold for Reconstructive Surgery. *Int. J. Mol. Sci.* **2015**, *16* (7), 14808−31.

(5) Gillies, A. R.; Lieber, R. L. Structure and function of the skeletal muscle extracellular matrix. *Muscle Nerve* **2011**, *44* (3), 318−331.

(6) Lieber, R. L. *Skeletal Muscle Structure, Function, and Plasticity*; Lippincott Williams & Wilkins, 2002.

(7) Grounds, M. D. Towards Understanding Skeletal Muscle Regeneration. *Pathol., Res. Pract.* **1991**, *187* (1), 1−22.

(8) Bischoff, R. Regeneration of single skeletal muscle fibers in vitro. *Anat. Rec.* **1975**, *182* (2), 215−235.

(9) Duffy, R. M.; Sun, Y.; Feinberg, A. W. Understanding the Role of ECM Protein Composition and Geometric Micropatterning for Engineering Human Skeletal Muscle. *Ann. Biomed. Eng.* **2016**, *44* (6), 2076−2089.

(10) Sun, Y.; Duffy, R.; Lee, A.; Feinberg, A. W. Optimizing the structure and contractility of engineered skeletal muscle thin films. *Acta Biomater.* **2013**, *9* (8), 7885−7894.

(11) Palchesko, R. N.; Szymanski, J. M.; Sahu, A.; Feinberg, A. W. Shrink Wrapping Cells in a Defined Extracellular Matrix to Modulate the Chemo-Mechanical Microenvironment. *Cell. Mol. Bioeng.* **2014**, *7* (3), 355−368.

(12) Palchesko, R. N.; Zhang, L.; Sun, Y.; Feinberg, A. W. Development of Polydimethylsiloxane Substrates with Tunable Elastic Modulus to Study Cell Mechanobiology in Muscle and Nerve. *PLoS One* **2012**, *7* (12), e51499.

(13) Duffy, R. M.; Sun, Y.; Feinberg, A. W. Understanding the Role of ECM Protein Composition and Geometric Micropatterning for Engineering Human Skeletal Muscle. *Ann. Biomed. Eng.* **2016**, *44* (6), 2076−89.

(14) Riboldi, S. A.; Sadr, N.; Pigini, L.; Neuenschwander, P.; Simonet, M.; Mognol, P.; Sampaolesi, M.; Cossu, G.; Mantero, S. Skeletal myogenesis on highly orientated microfibrous polyesterurethane scaffolds. *J. Biomed. Mater. Res., Part A* **2008**, *84* (4), 1094.

(15) Xu, C. Y.; Inai, R.; Kotaki, M.; Ramakrishna, S. Aligned biodegradable nanofibrous structure: a potential scaffold for blood vessel engineering. *Biomaterials* **2004**, *25* (5), 877−86.

(16) Sun, Y.; Jallerat, Q.; Szymanski, J. M.; Feinberg, A. W. Conformal nanopatterning of extracellular matrix proteins onto topographically complex surfaces. *Nat. Methods* **2015**, *12* (2), 134−6.

(17) Akhyari, P.; Kamiya, H.; Haverich, A.; Karck, M.; Lichtenberg, A. Myocardial tissue engineering: the extracellular matrix. *Eur. J. Cardiothorac Surg* **2008**, *34* (2), 229−41.

(18) Ott, H. C.; Matthiesen, T. S.; Goh, S. K.; Black, L. D.; Kren, S. M.; Netoff, T. I.; Taylor, D. A. Perfusion-decellularized matrix: using nature's platform to engineer a bioartificial heart. *Nat. Med.* **2008**, *14* (2), 213−21.

(19) Hong, X.; Yuan, Y.; Sun, X.; Zhou, M.; Guo, G.; Zhang, Q.; Hescheler, J.; Xi, J. Skeletal Extracellular Matrix Supports Cardiac Differentiation of Embryonic Stem Cells: a Potential Scaffold for Engineered Cardiac Tissue. *Cell. Physiol. Biochem.* **2018**, *45* (1), 319−331.

(20) Merritt, E. K.; Hammers, D. W.; Tierney, M.; Suggs, L. J.; Walters, T. J.; Farrar, R. P. Functional assessment of skeletal muscle regeneration utilizing homologous extracellular matrix as scaffolding. *Tissue Eng., Part A* **2010**, *16* (4), 1395−405.

(21) Valentin, J. E.; Turner, N. J.; Gilbert, T. W.; Badylak, S. F. Functional skeletal muscle formation with a biologic scaffold. *Biomaterials* **2010**, *31* (29), 7475−84.

(22) Wang, L.; Johnson, J. A.; Chang, D. W.; Zhang, Q. Decellularized musculofascial extracellular matrix for tissue engineering. *Biomaterials* **2013**, *34* (11), 2641−54.

(23) Wolf, M. T.; Daly, K. A.; Reing, J. E.; Badylak, S. F. Biologic scaffold composed of skeletal muscle extracellular matrix. *Biomaterials* **2012**, *33* (10), 2916−25.

(24) Modulevsky, D. J.; Lefebvre, C.; Haase, K.; Al-Rekabi, Z.; Pelling, A. E. Apple derived cellulose scaffolds for 3D mammalian cell culture. *PLoS One* **2014**, *9* (5), No. e97835.

(25) Gershlak, J. R.; Hernandez, S.; Fontana, G.; Perreault, L. R.; Hansen, K. J.; Larson, S. A.; Binder, B. Y.; Dolivo, D. M.; Yang, T.; Dominko, T.; Rolle, M. W.; Weathers, P. J.; Medina-Bolivar, F.; Cramer, C. L.; Murphy, W. L.; Gaudette, G. R. Crossing kingdoms: Using decellularized plants as perfusable tissue engineering scaffolds. *Biomaterials* **2017**, *125*, 13−22.

(26) Fontana, G.; Gershlak, J.; Adamski, M.; Lee, J. S.; Matsumoto, S.; Le, H. D.; Binder, B.; Wirth, J.; Gaudette, G.; Murphy, W. L. Biofunctionalized Plants as Diverse Biomaterials for Human Cell Culture. *Adv. Healthcare Mater.* **2017**, *6* (8), 1601225.

(27) Sun, Y.; Jallerat, Q.; Szymanski, J. M.; Feinberg, A. W. Conformal nanopatterning of extracellular matrix proteins onto topographically complex surfaces. *Nat. Methods* **2015**, *12* (2), 134−136.

(28) Feinberg, A. W.; Alford, P. W.; Jin, H.; Ripplinger, C. M.; Werdich, A. A.; Sheehy, S. P.; Grosberg, A.; Parker, K. K. Controlling the contractile strength of engineered cardiac muscle by hierarchal tissue architecture. *Biomaterials* **2012**, *33* (23), 5732−5741.

(29) Owens, J.; Moreira, K.; Bain, G. Characterization of primary human skeletal muscle cells from multiple commercial sources. *In Vitro Cell. Dev. Biol.: Anim.* **2013**, *49* (9), 695−705.

(30) Sun, Y.; Duffy, R.; Lee, A.; Feinberg, A. W. Optimizing the structure and contractility of engineered skeletal muscle thin films. *Acta Biomater.* **2013**, *9* (8), 7885−94.

(31) Bajaj, P.; Reddy, B., Jr.; Millet, L.; Wei, C.; Zorlutuna, P.; Bao, G.; Bashir, R. Patterning the differentiation of C2C12 skeletal myoblasts. *Integr Biol. (Camb)* **2011**, *3* (9), 897−909.

(32) Zatti, S.; Zoso, A.; Serena, E.; Luni, C.; Cimetta, E.; Elvassore, N. Micropatterning topology on soft substrates affects myoblast proliferation and differentiation. *Langmuir* **2012**, *28* (5), 2718−26.

(33) Modulevsky, D. J.; Cuerrier, C. M.; Pelling, A. E. Biocompatibility of Subcutaneously Implanted Plant-Derived Cellulose Biomaterials. *PLoS One* **2016**, *11* (6), No. e0157894.

(34) Miyamoto, T.; Takahashi, S.; Ito, H.; Inagaki, H.; Noishiki, Y. Tissue biocompatibility of cellulose and its derivatives. *J. Biomed. Mater. Res.* **1989**, *23* (1), 125−33.

(35) Martson, M.; Viljanto, J.; Hurme, T.; Laippala, P.; Saukko, P. Is cellulose sponge degradable or stable as implantation material? An in vivo subcutaneous study in the rat. *Biomaterials* **1999**, *20* (21), 1989−95.

(36) Entcheva, E.; Bien, H.; Yin, L.; Chung, C. Y.; Farrell, M.; Kostov, Y. Functional cardiac cell constructs on cellulose-based scaffolding. *Biomaterials* **2004**, *25* (26), 5753−62.

https://dx.doi.org/10.1021/acsbiomaterials.0c00058
ACS Biomater. Sci. Eng. 2020, 6, 3046−3054